LIDAR- DATA: AUTOMATIC OBJECT DETECTION TO SUPPORT URBAN FLOODING SIMULATION

MD. Aktaruzzaman, Theo G. Schmitt

Institute of Urban Water Management, University of Kaiserslautern, Paul Ehrlich strasse 14,
D-67663

mzaman@rhrk.uni-kl.de, tschmitt@rhrk.uni-kl.de

Commission I, WG I/3

KEY WORDS: LiDAR point cloud, Object segmentation, DSM, Surface runoff, Object detection

ABSTRACT:

Urban flooding is an increasingly alarming issue in terms of public safety and property damage. Climate change and its possible effects on the occurrence of more frequent extreme weather events have become an important topic in the area of global politics, science and engineering of today's world. The proper design of urban drainage systems and analysis of their hydraulic performance to secure flood protection in urban areas is a challenging task of urban water management. High resolution surface data describing hydrologic and hydraulic properties of complex urban areas is the prerequisite to more accurately describe and simulate the flood water movement and thereby to take adequate measures against urban flooding. LiDAR (Light detection and ranging) point cloud is an efficient way of generating high resolution digital surface model (DSM) of any study area. This paper presents an approach to segment LiDAR point cloud into ground and non-ground points based on slope change, height variation and standard deviation of neighbouring points. The non-ground points are later classified into buildings and trees by using an approach based on surface roughness and planar component calculation. Streets play an important role in terms of surface runoff generation. A semiautomatic approach has been developed to extract street point candidates from LiDAR data. A knowledge based expert system has been implemented to identify impervious surfaces (other than street) and grassland. Finally future ideas will be described to detect other surface drainage elements such as property boundary walls and slope information in the neighbourhood of the street as they are believed to guide the flood water flow and influence their possible intrusion into the private property (garage, basement).

1 INTRODUCTION

1.1 Motivation

The history of urban drainage goes back to some thousand years. Historical evidences suggest that ancient civilizations like Indus, Greeks and the Romans put as much importance to urban drainage as we do in our modern civilization. The Indus civilization flourished in the Indus river Valley in 3000 BC and Harappa and Mohenjo-Daro were the two important cities in this valley. Archaeological evidences and historical accounts revealed that this both cities were equipped with adequate urban drainage system in order to facilitate collection of rain water and conveyance of waste water and later transport them to Indus River. Similar evidences of urban drainage system have been reported in the Persian, the Mesopotamian Empire and the Minoan. People of the ancient civilization was well aware of the hazard of urban flooding and the necessity to drain out waste water and pollution to keep the living environment safe and healthy which in turn prompted them to design the drainage systems even centuries ago. The same spirit and philosophy of human civilization continued through medieval to the modern age. The urbanization process became massive and to cope up with the drainage facility, designing and maintenance of urban drainage system became more complex than ever before.

Conventional flood simulation models are not adequate enough to simulate the flood water flow phenomena in the urban area in case of excessive rainfall according to the requirement of European Standard EN-752 (Ettrich, 2005). Most of the models do not properly address the problem of the interaction of water between sewer and surface which resulted in inadequate handling of flooding scenario. The new methodology which is developed in the EUREKA-project RisUrSim (Schmitt, et al., 2004), solves this problem on the basis of shallow water equations solved on triangulated high resolution surface grids. Street inlets and manholes are assumed as the exchange nodes between the sewer and the surface which are located in the computational grid. Water that escapes the sewer during excessive rainfall is further propagated on the surface raising the demand of detailed surface information. Spatially densed topographical information is needed to build a model suitable for hydrodynamic runoff calculations in urban areas in addition to the detection of elements like houses, curbs, etc. that guide the runoff of water. Airborne data collection methods offer a great chance to economically gather densely sampled input data. The core focus of this research project is to construct detailed surface representation of a large area to support urban flooding. 'Dual drainage' is a term mostly used along with urban flood simulation techniques where pipe flow and surface flow are combined. A number of literatures are available describing this dual drainage urban flood simulation model. In most of the cases, these works either cover very small part of surface area (Street cross section) or relatively big area having lack of adequate integration of GIS and remote sensing technique. In today's research in the field of Geosciences, Hydrology and Environmental science integration of remote sensing and GIS technology has put an immense impetus of exploring every possible aspect. This research aims to integrate advanced remote sensing technology (airborne LiDAR data) and some forms of field data within GIS boundary to better visualize and characterize large urban area as accurately as possible. This is to mention that, the goal of the research work is to support urban flooding i.e., to make a supplementary platform with detailed information to represent surface of a large area which will

eventually act as an input to dual drainage flood simulation model.

1.2   Scope of the work

Urban Flooding has become an important issue in urban drainage planning and operation. The proper design of drainage systems and analysis of their hydraulic performance to assure or improve flood protection require accurate simulation models.

The existing urban flood modelling and simulation techniques are based on the detailed representation of the underground sewer network and the modelling of sewer flow is done by dynamic flow routing. At the same time, the surface data to describe relevant rainfall-runoff processes, being the driving force of urban flooding, are still very coarse. It has been recognized, however, that surface flow processes heavily affect the occurrence and extend of flooding both in terms of water levels and damage. Modeling of urban flooding therefore requires a more detailed representation of the catchment area on the surface. Available surface data, however, are extremely heterogeneous, fragmentary and highly unstructured. Requiring innovative and efficient methods of data mining and processing, visualization techniques are a promising approach to generate an adequate data base for modeling and simulation of urban flooding (Aktaruzzaman, M. and Schmitt, T., 2009).

The concept of urban drainage through minor system, i.e., underground pipes and major system, i.e., parts of street cross-section was introduced in the eighties in North America (Djordjević, S. et al., 2004). The interaction of water between this major and minor system through a guided way is popularly know as dual drainage

In the meantime advancement has been made in the flood simulation techniques and there has been significant development in the data acquisition technologies which have enabled detailed, explicit and accurate handling of minor-major system reaction (Tomičić et al., 1999 ; Prodanović, 1999). The introduction of GIS based technologies in addition to improved simulation techniques have helped designing technically sound minor-major system which resulted in more reliable urban flooding simulation and realistic estimation of the consequences (Schmitt et al., 2002).

1.3   Related Work / Literature Review

There are literatures available describing urban flood modelling using LiDAR data. Most of them deal with river flooding. Abdullah et al., (2009) described DTM generation process by using open source software ALDPAT. They excluded buildings, bridges and trees before applying flood simulation model. Tsubaki and Fujita (2010) generated detailed surface model from LiDAR to feed it into flood inundation modelling. Their work focuses on river flooding and presents an efficient way to generate unstructured gridded representation of the urban topology. Haile and Rientjes, (2005) described the sensitivity of LiDAR DEM resolution on urban flood modelling.

 In our research work we are particularly aiming at urban flooding caused by excessive rainfall and seasonal storms causing failure to existing drainage capacity. Flood inundation modelling is not the scope of the study but to better support the

inundation modelling by generating high spatial resolution surface data with objects detailing and surface characterization. Schmitt et al., (2004) introduced the concept of urban surface detailing in a small area and connected it to urban drainage modelling. They generated high resolution surface data of a small street area by manual data collection. Ettrich (2007) described detailing of complex urban areas including subtle surface distinction such as street, curbs and sidewalls. He extracted buildings and streets from LiDAR data manually by giving polygonal inputs.

In our research work emphasis has been given on automatic filtering of LiDAR data followed by automatic object classification. Liu (2008) presented literature works related to LiDAR data for DEM generation. LiDAR data is a convenient source from where digital terrain information can be made. Raber et al., (2007) described that LiDAR data have become prominent source of information to generate digital terrain model and have been used in urban modelling and hydrological modelling. Hodgson et al., (2005) described that the main purpose of LiDAR data collection has been to generate terrain modelling. Forlani and Nardinocchi (2007) also described the same importance. Hodgson and Bresnahan (2004) showed that people of spatial science is not only preferring but also making it a standard practice to generate terrain model from LiDAR data. Curiosity may arise, since when people have been using LiDAR data? According to Flood (2001), since 1960s people have been using it. Bufton et al., (1991) and krabill et al.,(1984) described that research on LiDAR system to collect topographic data started from 1980s. According to Pfeifer and Briese (2007), LiDAR system emerged commercially in mid 1990s. With the gradual improvement and development in LiDAR system , its users community has also increased. Sithole and Vosselman (2003) described that over the last decade there has been a significant increase in the use of LiDAR data for digital elevation model generation. Many authors , such as Lloyd and Atkinson (2002), Wack and Wimmer (2002) and Kobler et al., (2007) described the application of LiDAR to generate terrain model in different example cases.

Airborne LiDAR data falls under the category of active remote sensing. LiDAR data has advantage over traditional photogrammetry for DEM generation specially in urban and forest areas as LiDAR sensor takes data from single sensor while for photogrammetry it is necessary to view the area from two locations. Stoker et al., (2006) and Barber and Shortrudge (2004) described that LiDAR pulse returns not only from buildings and tress but also from power lines, telephone polls and birds. But bare earth points are always topic of interest to generate DTM. That is why, it is an important task to filter or extract bare earth points from LiDAR data. Many filter methods have been developed to classify or separate raw LiDAR data into ground and non-ground points. Romano (2004) described that almost none of the filtering algorithm is 100% accurate. Chen (2007) showed that manual interaction is still needed to improve filtering algorithms. LiDAR technology is growing in fast pace and large amount of data acquired by this technology must be handled in an efficient way. Sangster (2002) described that high density LiDAR data has increased the data volume and has created challenges in terms of data storage, processing and interpretation. Chen (2007) described that gradual drop of the cost of LiDAR data has made it popular and convenient for the users.

2 MATERIALS

The study area was part of Kaiserslautern University and its surroundings. Raw LiDAR (light detection and ranging) data having spatial resolution of 0.25 meter was acquired form BSF SwissPhoto. It means that the density of the LiDAR point cloud is 4 points per square meter which is sufficient enough to describe many small surface properties apart from buildings and big objects. Other available supporting data are city polygon maps of buildings and streets, aerial imagery of 10 cm spatial resolution. Figure 1 shows the aerial image of the study area.
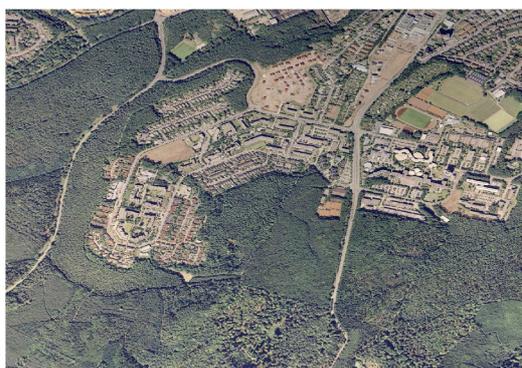
Figure 1: Aerial image of the study area

3 METHODOLOGY

3.1 Object Extraction

Filtering is the process of separating off-terrain points (buildings, trees and other objects) from on-terrain points (DTM). A moving window based spatial filter has been designed based on slope change, height variation and standard deviation of neighbouring points in the raw LiDAR point cloud. In LiDAR community filtering generally means 'morphological filtering'. Morphological filtering is operated only on the grid data (image pixels). This morphological filtering is a special type of classification where the main objective is to classify LiDAR data into two classes, namely ground and nonground points (Vosselman, 2000). The ground data points are used for generating DTM and the nonground points are used for object detection and subsequent classification. Shan and Sampath (2005) described a filter mainly for urban areas. It determines the nonground points along the LiDAR scan line. There are many morphological filters that have been developed to separate ground and nonground points are based on the characteristics such as elevation and slope difference of LiDAR points. Zhang and Whitman (2005) developed a filtering method based on elevation threshold. Vosselman (2000) developed a slope-based filter. Some researcher introduces new techniques in their filtering algorithm. Haugerud and Harding (2001) proposed a filter based on local curvature whereas Passini and Jacobsen (2002) presented a filter based on linear prediction method. In this paper a new filtering algorithm has been proposed which is not a morphological type filtering, rather a kind of spatial filtering operated on raw LiDAR point cloud. Besides considering elevation and slope criteria of ground points, partitioning of point data along Z direction (Height) on a neighbourhood scale and special security checking to confirm

the first point as either ground or nonground. The special security checking involves calculation of standard deviation of the points in each partitioned layer. The variation of standard deviation up to a specific threshold and position of the first point confirms itself as ground or nonground point. Shan and Sampath (2005) assume the first point as ground point and validate the assumption by one-dimensional bidirectional filter. The partitioning of LiDAR points along the height on neighbourhood scale gives the intuitive proportional distribution of ground and nonground points and their number ratio. This information along with slope and height criteria helps better to classify points when some parts of the urban area have really complex pattern with varying and erratic object shapes and heights.
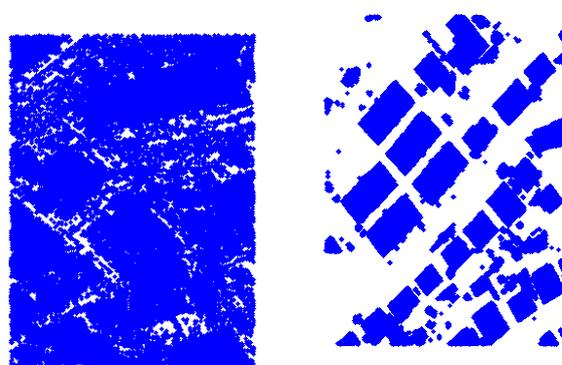

Figure 2: Objects (Buildings and Trees) extraction from LiDAR point cloud. Figure at the left shows unstructured LiDAR data and figure at right shows extracted objects.

Taking object points out of the point cloud and filling those gaps with appropriate interpolation method is a way to generate digital terrain model (DTM). Placing the extracted objects again on the DTM gives birth to the tern DSM (Digital surface model). The objective of object separation and subsequent classification of buildings and trees was to support the idea that the rain water falling on the roof top will go directly to the sewers and in case of trees there will be initial moistening and interception before the water touches ground. Figure 2 shows raw LiDAR point cloud (left) and the extracted objects (right) after applying our filtering algorithm.

3.2 Object Clustering

After extraction of non ground objects from LiDAR point cloud, attention was paid to the classification of the objects. Work has been done on the separation of buildings and vegetation. Most of the works use a variety of dataset such as infrared imagery, colour imagery, LiDAR data and combine them together to separate the objects.

Several studies have shown that LiDAR data has the potential to support 3D feature extraction, especially if combined with other types of data such as 2D GIS ground plans (Brenner and Haala,

1999; Weidner and Förstner, 1995). The calculation of DTM from a DSM with the help of image matching is describes in Passini and Jacobson (2002). The use of reflectance-based identification is described in Hug (1997). Oude Elberink & Maas (2000) describes the use of anisotropic height texture such as the co-occurrence matrix and contrast texture measures in LiDAR data used for unsupervised classification. This method allows to remove the vegetation. In this work an attempt has been made to separate buildings and trees from LiDAR point cloud only. The algorithm is based on the idea 'to make packet of all visible clusters' and later an individual treatment was applied to each of the cluster to recognize their patterns in terms of building and tree.
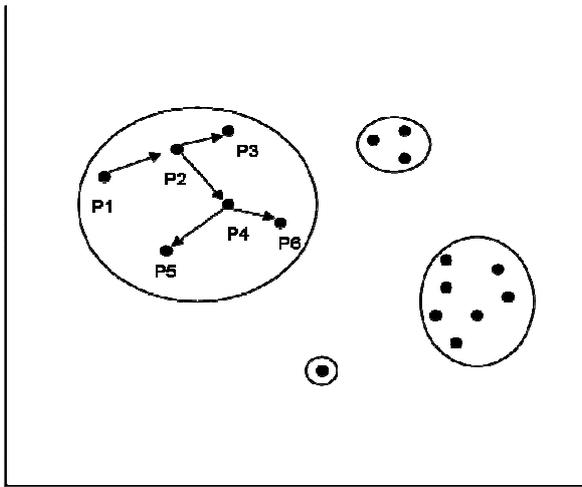

Figure 3: Automatic object clustering technique

The algorithm starts with the first numerical point of the dataset supplied as text (*.txt) file to the system. Let the point be P1. P1 searches the nearest point P2 within a given threshold value. Then P2 searches its nearest point P3 within the threshold and stores all the points in a packet until the last point Pn does not find any point within given proximity. The formation of a 'cluster packet' is thus completed and the algorithm then fixes the next point sequentially from the text file list and allows it to grow into a new cluster. When the point P1 does not find any point in its threshold proximity, it makes a cluster in itself. After making segmentation of all the visible clusters, each of the 'packet clusters' was investigated. Figure 3 shows the automatic object clustering technique.

3.3 Object Classification by Pseudo gridding approach

The object clustering approach not only 'packets' an object but also gives each packet a numerical identity. This numerical identity helps better classify the object followed by the 'Pseudo gridding' algorithm. Pseudo gridding is an approach to break the whole objects into small square blocks (Figure 4). Then each of the small grids was checked to designate that grid as either 'building' or 'tree'. Height profile and standard deviation of z values (height) of the points within a grid were the criteria

that were investigated for each grid. A given threshold of height difference and standard deviation assign each grid as either building or tree. The assumption behind this checking is that tree surfaces have more irregular height profile whereas building surfaces have regular height profile. This is only the general assumption. Many roof tops have an irregular surface due to the presence of chimney, solar panel or water tank. Normally sloped roofs also have smooth surfaces which can be detected by pseudo grid approach. But situation turns complex
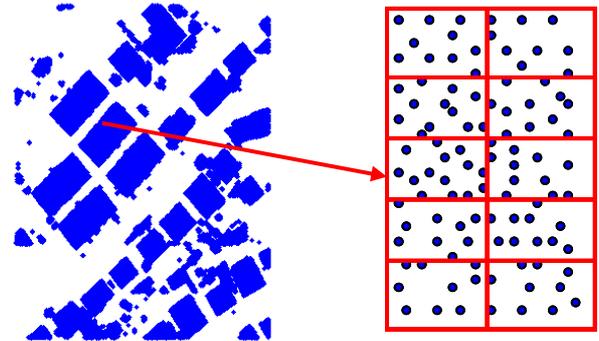

Figure 4: Concept of Pseudo Gridding

when trees and buildings are attached together or even worse when trees overhang on the buildings. Pseudo grid is an efficient approach to separate buildings and trees even when they are attached together. Breaking down the whole cluster object into smaller parts help to draw satisfactory partition between building and tree. The pseudo grid approach is not an absolute error free algorithm. Sometimes particular grid shows anomalous behaviour being a part of same object. This type of cases requires some adjustment as shown in Figure 6.
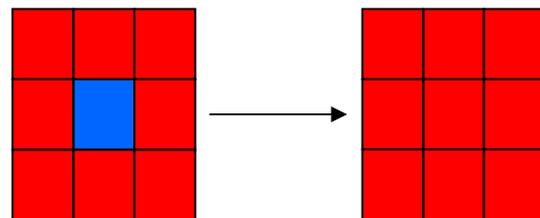

Figure 5: Final decision objects after grid adjustment

In figure 5 (left) the presence of blue grid (tree) in the middle surrounded by red grids (building) is a weird representation of the whole object as building. The presence of chimney or water tanks have resulted in rough surface and height change more than threshold set for detecting building object. An automatic adjustment has been implemented to handle this kind of situation. The automatic adjustment algorithm is based on the idea that any grid takes on the property of neighbouring grids. Thus in figure 5, the central blue grid has been adjusted as red grid following the existence of surrounding red grids. Figure 6 shows the object classification followed by pseudo gridding algorithm of the whole study area where red represents building candidate points and blue represents tree point candidates.

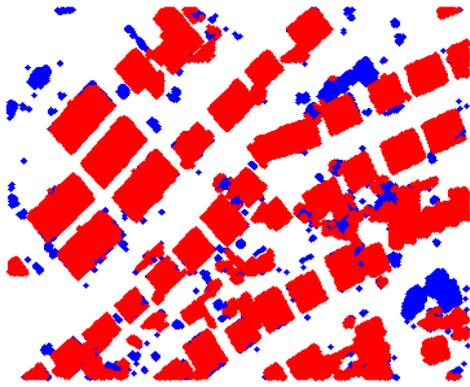Figure 7: Object cluster classified as tree (blue) after pseudo gridding.

Figure 6: Object classification after pseudo gridding in the point cloud (Building (red) and tree (blue)).

3.4 Classification refinement by planar analysis

Planar analysis follows the pseudo grid approach and attempts to capture the planar information of an object cluster. Some object cluster has highly heterogeneous point cloud distribution. For example, when any object cluster contains one building and more than one tree and thus the relative volume of tree point cloud is large, in that specific case pseudo gridding performs poorly. Planar analysis is a method based on principal component analysis to identify flat regions in a point cloud. A principal component analysis of a given set of points in 3D point cloud shows the direction of mutually orthogonal vectors (eigenvectors) and their relative strength (eigenvalues) (Shan and Sampath , 2005). If a set of points has two dominant eigenvalues and the third value is nearly zero, those points said to be on a plane. Let a set of points M be denoted by X_i

(i=1,………….., m) and let $\overline{X}$ be their mean vector. The covariance matrix is calculated as:

$$\sum_{XX} = \sum_{i=1}^{m} (X_i - \overline{X})(X_i - \overline{X})^T \qquad (1)$$

The eigenvalues λ_1, λ_2, λ_3 and their corresponding

eigenvectors Λ_1, Λ_2 and Λ_3.

If $[\lambda_1 / (\lambda_1 + \lambda_2 + \lambda_3)] < \xi$, then set of points M is planar,

where ξ is a small number. Figure 7 shows one object cluster with apparently three objects attached together. Because of its highly unstructured pattern pseudo gridding failed to distinguish building and tree and treated the whole object as tree.
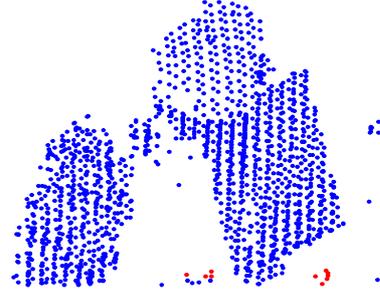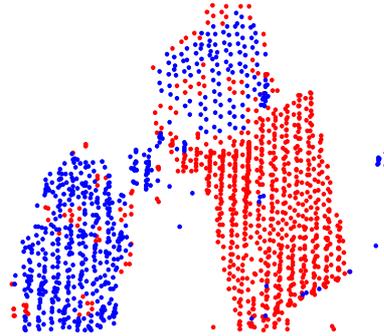

Figure 8: Object cluster classified as building (red) and tree (blue) after planar analysis.

In figure 8, it is clear that same object cluster has been classified into building and trees after applying planar analysis method.

3.5 Spectral information integration

Spectral information integration (SII) technique involves mapping spectral value from image pixel to LiDAR point data. This is an approach of exploiting spectral information from image pixel and then to correct the misclassified points in an object clusters (if there is any). Consecutive application of pseudo gridding and planar analysis classified most of the object cluster accurately with the exception of few object clusters. Figure 9 shows the classified buildings and trees in the study area after applying planar analysis algorithm.
These exceptional clusters were both building cluster having few misclassified points inside it and tree clusters showing sudden flat zone on the edge. The reason could be the presence of several chimneys and dormer windows on one rooftop and a sudden flat region at the edge of any tree object.
SFI methodology attempted to identify those points first by looking at the geographic coordinates of those misclassified points. As both the LiDAR point cloud and the aerial image were geo-referenced to same coordinate system (Gauss Kruger-3), linking the misclassified points to the corresponding image pixels was done through an automatic routine.
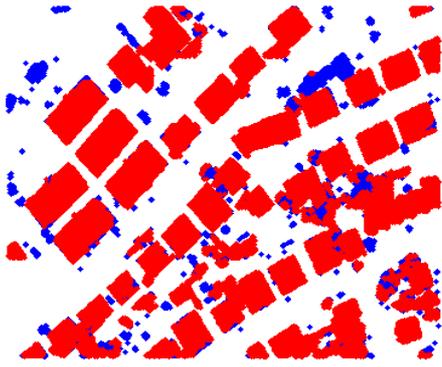
Figure 9: Object classification after pseudo gridding and planar analysis in the point cloud (Building (red) and tree (blue)).

A colour index (CI) was calculated for each pixel and a threshold value of that colour index was chosen that could distinguish building and tree on spectral basis. The formula of the CI is as,

$$CI = (green/ \; red + green + blue) \qquad (2)$$
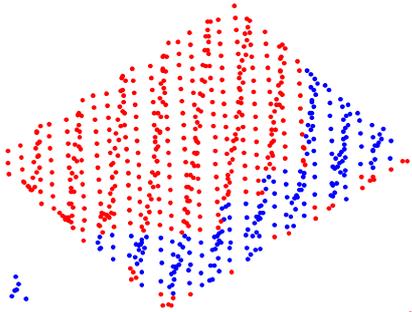

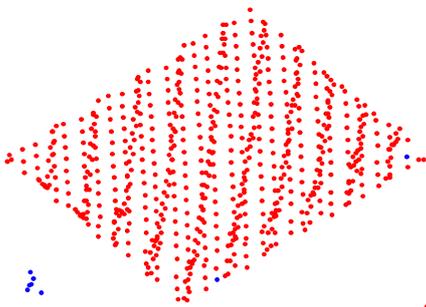Figure 10: Building object before applying SFI technique

Figure 11: Building object after applying SFI technique

It was investigated that, CI value less than 0.35 corresponds to building pixel whereas CI value equal or more than 0.35 corresponds to tree pixel. In figure 10, a building object

contains mixed type of points namely building points (red) and tree points (blue). In figure 11, the same building object has been cleaned automatically after the application of SII algorithm.

4 RESULT AND ACCURACY

The final result of the classified map after applying pseudo gridding, planar analysis and spectral information integration is shown in figure 12. To determine the accuracy of the classified map, an error matrix was computed. An error matrix is a matrix
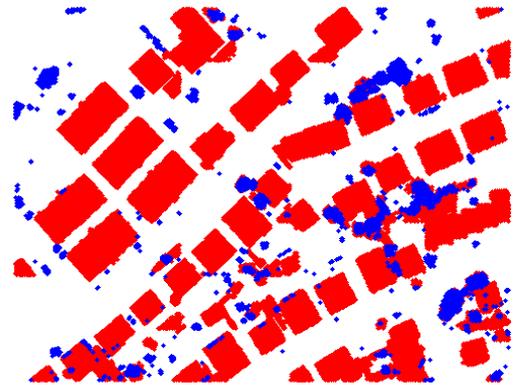

Figure 12: Object classification after pseudo gridding, planar analysis and spectral integration approach in the point cloud (Building (red) and tree (blue)).

Figure 13: Aerial image of part of the study area where object classification was investigated

or table that displays statistics for assessing image classification accuracy by showing the degree of misclassification among classes (Glossary of remote sensing terms, Canada centre for remote sensing). The error matrix is a way to compare two

thematic maps, one a 'ground map' (the reference map) and the other is a map produced by automatic classification algorithm (the classified map). In our case the reference map was the orthophoto of the study area in the figure 13 and the classified map was the final product of the classified LiDAR point cloud showed in figure 12.

Classified map	Reference map		
		Building	Tree	Ground
	Building	87	1	5
	Tree	3	20	2
	Ground	2	1	179

Table 1: Error matrix of the classified map against reference map

Overall accuracy = (87+20+179)/300
= 95.33 %

	Building	Tree	Ground
User's accuracy (%)	93.5	80	98.35
Producer's accuracy (%)	94.57	90.91	96.24
Errors of omission (%)	5.43	8.09	3.66
Errors of commission (%)	6.5	20	1.65

Table 2: Calculation of different accuracies

Table 1 shows the error matrix of the classified map against reference map and table 2 shows the calculation of user's accuracy, producer's accuracy, errors of omission and errors of commission. The overall accuracy turned out to be 95.33%.

5 STREET EXTRACTION

Street detection on the Digital surface model is an important and necessary task for the preparation of a detailed surface database to simulate flooding phenomena in urban areas. Street surface is a place where runoff occurs and interaction between sewer and surface water takes place. Manholes and water inlets are the gateway that facilitates these interaction phenomena making the concept of urban flooding characteristic. Another important emphasis of this research is the detailing of streets, sidewalks and the height of the curbs. Usually height of the curbs range from 5 to 10 cm. At the same time LiDAR data has vertical accuracy of 3 to 5 cm. It is a challenging task to determine the curb height accurately because in many places the curb height is too small or there is no curb at all. The curb height is important in simulation model because of the location of street inlets and the possible entering of the water from the street to the private ground. Street inlets are located at the foot of curb wall. In case the street inlets are located on the top of curb wall by mistakes, flood modelling is going to be affected. Road extraction from LiDAR data is not a new idea. In fact some works has been done on this issue. Researchers have adopted two approaches namely automatic and semi-automatic approaches to detect road in the LiDAR data. In automatic approaches, people have mostly followed the conventional way in computer vision. It means converting the LiDAR point cloud into gray scale image as a first step, later applying digital image processing technique on the gray scale image. In semiautomatic approaches people have tried to combine existing vector road maps and raster LiDAR image to detect road network. In this paper a semiautomatic approach for detection of road has been described. This approach combines the vector data and raw LiDAR point cloud without converting it into gray scale image or any other raster format. The idea behind this approach is that raw points preserve the originality of the surface before they are converted to any other formats. At first the centreline of the road network from vector maps are collected. Taking this centreline as seed point's information, road points are extracted from LiDAR point cloud. The road extraction algorithm actually encapsulates the points in both sides of the centreline. The point searching region is limited by the input of the road boundary lines from road polygon maps. The centrelines are provided as point data as input to this algorithm. In Figure 14, a street segment is consisted of three points $O(x_0,y_0)$, $O_1(x_1,y_1)$ and $O_2(x_2,y_2)$. The algorithm starts with $O(x_0,y_0)$ and searches for point Q and P on both sides of O respectively by using simple trigonometric formula $dx=r\cos(\theta)$ and $dy=r\sin(\theta)$. The value of r is the distance between centreline and the intersecting point of road boundary and OQ. Same procedure is followed to search the points Q1 and P1. A search algorithm is implemented to extract the points bounded by the rectangle PQQ1P1. The street extraction algorithm is guided by points on the centreline and goes for drawing next rectangle P1Q1Q2P2 and subsequently extracting points bounded by that rectangle. Figure 15 shows the final stage of road extraction and closer view at the road candidate points.
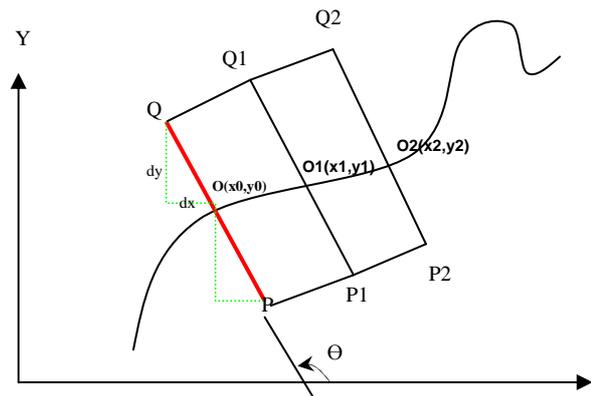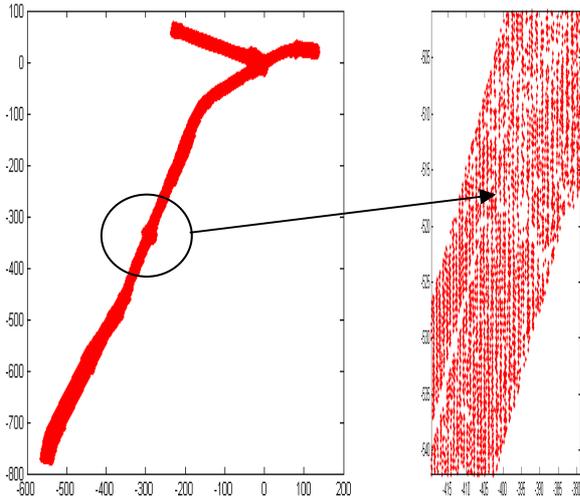

Figure 14: Street extraction

Figure 15: Street candidate points after extraction from LiDAR data

6 IMPERVIOUS SURFACE DETECTION

Impervious surfaces such as surfaces having concrete and asphalt layer on top do not allow water to percolate through them. In case of precipitation, this surface produces maximum runoff leading the water into drainage network. As urban flooding mainly caused by 'rainfall overwhelming drainage capacity', that is why proper identification of impervious surfaces is an important task to model urban flooding. Urbanization helps grow amount of impervious surfaces. Many local, state and federal regulations have attempted to limit the development of impervious surfaces by adjusting zoning regulations (Hodgson et al 2003). Some local jurisdictions apply a stormwater levy (tax) based on the size and percentage of a parcel that is impervious (Kienegger, 1992). Therefore an accurate method to detect impervious surface is also useful for proper planning, design and urban economic factors. Considerable remote sensing research has focused on accurately mapping impervious surfaces. Ridd (1995), Ji and Jensen (1999), and Wu and Murray (2002) mostly used statistical classification approaches with moderate resolution satellite imagery. Hodgson, et al., (2003) used high resolution aerial image and LiDAR height data.

In this work, a knowledge based expert system (KBES) has been implemented to detect impervious areas using high resolution aerial image (10 cm by 10 cm) and LiDAR intensity data unlike Hodgson, et al., (2003).Figure 16 shows the study area where the KBES system was implemented. An object-based image segmentation is the pre-requisite to apply any knowledge based classifier in our method. The term 'segmentation' means subdividing objects into smaller partitions. Chessboard segmentation was applied by using definiens 8.0 (Definiens, 2010). Chessboard segmentation algorithm breaks the image object into equal squares of a given size. Chessboard algorithm in the definiens can also be guided by providing external vector maps which help break the image

according to input vector objects instead of equal sizes square. Figure 17 shows the external vector map of the city parcel. This option in definiens was utilized to segment the image of the study area according to the boundary lines of the parcel map of the same area. Figure 18 shows how the aerial photo of the study area has been segmented followed by the application of chessboard segmentation. Chessboard segmentation is in fact not truly object based segmentation.

Figure 16: Aerial image of part of the study area

Figure 17: City parcel map of the study area

Object-based segmentation takes into account the homogeneous pixels in neighbourhood basis and forms image primitives. Multiresolution segmentation satisfies the purpose of object-based segmentation and it was carried out as a second step segmentation after performing chessboard segmentation. Multiresolution segmentation breaks each segmented parcel object into homogeneous object primitives. The size of these primitives can be controlled by user defined shape and size factor in definiens. The software also has option for assigning different weights to different wavebands. Figure 19 shows Multiresolution segmentation and example decision rule for image objects classification.

Figure 18: Chessboard segmented image

If (blue < 125) AND
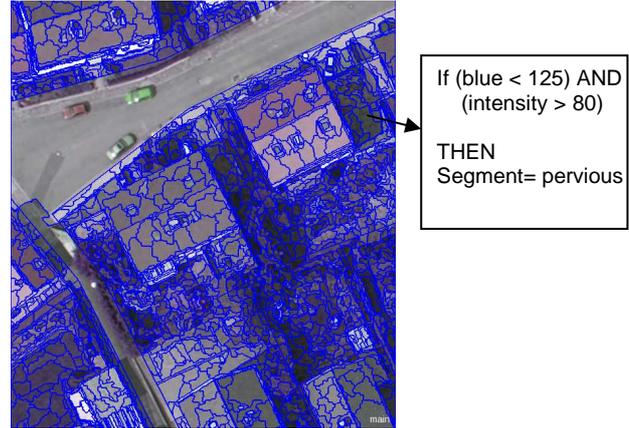(intensity > 80)

THEN
Segment= pervious

Figure 19: Multiresolution segmentation and example decision rule for image objects classification.

When the image segmentation is complete, we still do not know the properties or features of each segmented object and also which objects belong to which classes. Studying and investigating the properties/ features of each segmented objects are the initial steps before developing knowledge based rule sets. Features or properties of a segmented image object are attributes representing specific information of that particular segmented object.

Definiens software provides two types of classifiers for assigning class labels to each segmented objects. They are rule set based classifier and nearest neighbour classifier. In this work rule set based approach has been opted for. In rule set approach one can define rules by using expert knowledge to guide the classification process. The datasets used in this work were aerial image and LiDAR intensity data. The aerial image has 0.1 m spatial resolution with three colour channels, blue, green and red. Our rule based approach targets to identify two land cover types, pervious and impervious. As street/road has already been detected, we excluded them from the search domain inside the whole image. The total number of wavebands used for rule set development was seven namely three wavebands from RGB image, three PCA bands computed from RGB image and LiDAR intensity band. We determined that mean values of layer 3 (blue band of RGB) can distinguish most of the buildings including garages and some paved surfaces attached to buildings. Mean values of layer 4 (LiDAR intensity band) could capture pervious surfaces (e.g., grassland, soil and bush) of the study area including the grassland under shadow after setting a threshold value. The rest of the unclassified areas (mainly impervious area under the shadow) were identified with PCA band 3 feature with a suitable investigated threshold value.

Figure 20 shows the classified pervious and impervious areas.
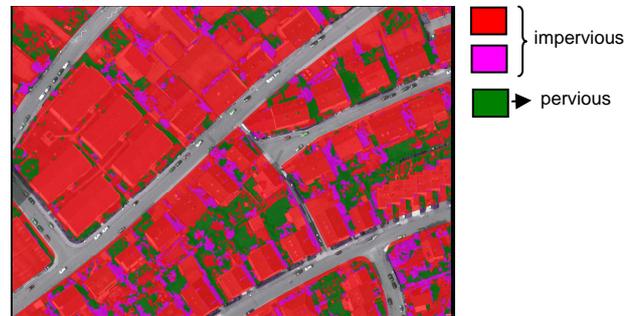

impervious

pervious

Figure 20: Classified pervious and impervious area.

7 FUTURE IDEAS

One of the objectives of this research work is to generate detailed urban surface representation as accurately as possible. Detection of macro objects such as buildings, trees and streets from LiDAR data alone or with the help of multispectral images has been a research topic for a decade. On the other hand, very few works have been done to detect micro objects such as street and pavement curbs, property boundary walls and fences next to the street. Abdullah, A.F., et al (2009) described the detection and construction of micro objects such as street divider and ramps by giving city GIS data as polygonal input which is not an automatic process. In this work we are aiming at detecting street curbs, boundary walls, fences and slope information in the street neighbourhood in an automatic way with the help of LiDAR and multispectral image. Research work is in progress on how to develop a framework based on wavelet analysis and tensor voting approach to detect break lines due to the presence of street curbs and boundary walls.

8 CONCLUSION

This paper has presented an innovative but simple LiDAR filtering algorithm to separate on-terrain and off-terrain points. This paper also presents an object clustering algorithm to facilitate classification process, pseudo gridding algorithm to classify objects followed by planar analysis and spectral information integration techniques in an automatic manner. It is necessary to mention here that object extraction from point cloud data was done through designing a moving window based spatial filter. Like many other filtering algorithms, it searches object on the basis of height information but with the exception of additional height partitioning and standard deviation criteria. The object clustering algorithm is based on the concept of linear distance calculation among points within a certain threshold to put them into a 'Packet' or 'Cluster'. The pseudo gridding algorithm breaks the cluster down to small square grid and then checks the height profile of each grid in order to designate the whole cluster either as building or tree. The resulted classification by pseudo gridding was further refined by planar analysis and spectral information. Street extraction from LiDAR data was done through a GIS database guided approach which was actually a semiautomatic algorithm. A knowledge based classifier was designed to detect pervious and impervious surfaces. Finally future ideas have been discussed on how to detect other micro objects on the urban surface elevation.

References

Abdullah, A.F., Rahman, A.A. and Vojinovic, Z. ISPRS Working Group III/2, Point Cloud Processing. Paris, France, September 2009.

Aktaruzzaman, M. and Schmitt, T.: Detailed Digital Surface Model (DSM) Generation and Automatic Object Detection to Facilitate Modeling of Urban Flooding. ISPRS Workshop , Hannover 2009.

Barber, C.P. and Shortrudge, A.M. 2004: Light detection and ranging (LiDAR)-derived elevation data for surface hydrology applications. East Lansing, MI: Institute of Water Resource, Michigan State University.

Brenner, C. and Haala, N., 1999: Rapid acquisition of virtual reality city models from multiple data sources. IAPRS, Vol. XXXII, Part 5, pp 323-330.

Bufton, J.L., Garvin, J.B., Cavanaugh, J.F., Ramos-lzquierdo, L., Clem, T.D. and Krabill,
W.B. 1991: Airborne lidar for profiling of surface topography. Optical Engineering 30, 72–78.

Chen, Q. 2007: Airborne LiDAR data processing and information extraction. Photogrammetric Engineering and Remote Sensing 73, 109–12.

Definiens, 2010. eCognition 8.0 User Guide(Object oriented Image classification software), Definiens Imaging GmbH, München, Germany.

Djordjevic, S., Prodanovic, D., Maksimovic, C. and Savic, D.: SIPSON – Simulation of Interaction between Pipe flow and Surface Overland flow in Networks. Int. Conference on Urban Drainage Modelling, Dresden 2004, pp. 115-124

Ettrich,N. (2005).Generation of Surface Elevation Models for Urban Drainage Simulation, Bericht des Fraunhofer ITWM, Nr. 79 (2005).

Ettrich, N. 2007; Surface-sewer coupling and detailed elevation models for accurate urban drainage modelling. In Proceedings Cost Session Aquaterra Conference 2007, Special Aspects of urban flood managements, pp. 183-196.

Forlani, G. and Nardinocchi, C. 2007: Adaptive filtering of aerial laser scanning data. International Archives of Photogrammetry, Remote Sensing and Spatial Information Sciences 36(3/W52), 130–35.

Flood, M. 2001: Laser altimetry – from science to commercial lidar mapping. Photogrammetric Engineering and Remote Sensing 67, 1209–11, 1213–17.

Glossary of remote sensing terms, Canada centre for remote sensing.
http://www.ccrs.nrcan.gc.ca/glossary/index_e.php?id=3124(accessed 28 March, 2010).

Haile, A. T. and Rientjes, T. H. 2005: Effects of LIDAR DEM resolution in flood modelling. A model sensitivity study for the city of Tegucigalpa, Honduras. ISPRS Workshop 'Laser scanning 2005', Enschede, The Netherlands, September, 2005.

Hodgson, M.E., Jensen, J., Raber, G., Tullis, J., Davis, B.A., Thompson, G. and Schuckman, K. 2005: An evaluation of LiDAR-derived elevation and terrain slope in leaf-off condition. Photogrammetric Engineering and Remote Sensing 71, 817–23.

Haugerud, R.A. and D.J. Harding, 2001. Some algorithms for virtual deforestation (VDF) of LIDAR topographic survey data, Int. arch. Photogrammetry and Remote sensing, XXXIV, Part 3/ W4: 219-226.

Hodgson, M.E., Jensen, J.R., Tullis, J., Riordam, K.D., and Archer, C.M., 2003. Synergistic Use of LiDAR and Color Aerial Photography for Mapping Urban Parcel Imperviousness. Photogrammetric Engineering and Remote Sensing, 69(9):973-980.

Hodgson, M.E. and Bresnahan, P. 2004: Accuracy of airborne lidar-derived elevation: empirical assessment and error budget. Photogrammetric Engineering and Remote Sensing 70, 331–39.

Hug, C., 1997: Extracting artificial surface objects from Airborne Laser Scanner Data. In: Automatic extraction of Man-Made Objects from Aerial and Space Images (II), A. Grün, E. Baltsavias and O. Henricsson (eds). Birkhaüser Verlag, Basel, pp 203-212.

Ji, M., and J. R. Jensen, 1999. Effectiveness of subpixel analysis in detecting and quantifying urban imperviousness

from Landsat Thematic Mapper Imagery. Geocarto Interantional,14(4):31-39.

Kienegger, E.H., 1992. Assessment of a wastewater service charge by integrating aerial photography ad GIS. Photogrammetric Engineering and Remote Sensing 58(11); 1601-1606.

Krabill, W.B., Collins, J.G., Link, L.E., Swift, R.R. and Butler, M.L. 1984: Airborne laser topographic mapping results. Photogrammetric Engineering and Remote Sensing 50, 685–94.

Kraus, K & Pfeifer, N., 1998. Determination of terrain models in wooded areas with airborne laser scanner data. ISPRS Journal of Photogrammetric and Remote Sensing, Vol. 53, 1998.

Kobler, A. and Ogrinc, P., 2007. Rein Algorithm and the influence of point cloud density on nDSM and DEM precision in a Submediterranean forest. ISPRS Workshop on Laser Scanning and SilviLaser 2007, Espoo, September 12-14, 2007, Finland.

Lemmens, M., 2007. Airborne Lidar Sensors. GIM International, 21(2).

Liu, X. (2008). Airborne LiDAR for DEM generation: Some critical issues. Progress in Physical Geography 32(1), pp. 31-49.

Lloyd, C.D. and Atkinson, P.M. 2002: Deriving DSMs from LiDAR data with kriging. International Journal of Remote Sensing 23, 2519–24.

Martinoty, G., 2003, Materials' BRDF retrieval from multiview digital aerial images. Geoscience and Remote Sensing Symposium 2003, IGARSS '03, Proceedings. 2003 IEEE International, 6, pp. 3851-3853.

Meister, G., Rothkirch, A., Spitzer, H., Bienlein, J., 2000, BRDF field studies for remote sensing of urban areas. Remote Sensing Reviews, 19, pp. 37-57.

Oude Elbernik, S. and Maas, H.G., 2000: The use of anisotropic height texture measures for the segmentation of airborne laser scanner data. IAPRS, Vol. XXXIII, Part B3/2, pp 678-684.

Passini, R., and K. Jacobson, 2002. Filtering of digital elevation models, Proceedings of the ASPRS annual convention, 19-26 April, 2002.

Pfeifer, N. and Briese, C. 2007: Geometrical aspects of airborne laser scanning and terrestrial laserscanning. International Archives of Photogrammetry, Remote Sensing and Spatial Information Sciences 36(3/W52), 311–19.

Prodanvic, D. 'Improvements of application methods in analysis of runoff from urban areas'. PhD thesis presented at the University of Belgrade, Yugoslavia, November 1999.

Raber, G.T., Jensen, J.R., Hodgson, M.E., Tullis, J.A., Davis, B.A. and Berglend, J. 2007: Impact of LiDAR nominal post-spacing on DEM accuracy and flood zone delineation. Photogrammetric Engineering and Remote Sensing 73, 793–804.

Richter, R., Schläpfer, D., 2002, Geo-atmospheric processing of airborne imaging spectrometry data. Part 2: atmospheric /topographic correction. International Journal of Remote Sensing, 23(13), pp. 2631-2649.

Ridd, M.K., 1995. exploring a V-I-S (vegetation-impervious surface-soil) model for urban ecosystem analysis through remote sensing-comparative anatomy for cities. International Journal of Remote Sensing, 16(12):2165-2185.

Romano, M.E. 2004: Innovation in LiDAR processing technology. Photogrammetric Engineering and Remote Sensing 70, 1202–206.

Tsubaki, R. and Fujita, I., 2010. HYDROLOGICAL PROCESSES, published online in Wiley InterScience. http://www3.interscience.wiley.com/cgibin/fulltext/123285257/PDFSTART(accessed 20 March, 2010).

Sangster, C. 2002. Validating LiDAR - evaluating LiDAR accuracy using GPS. Lawrencetown , Nova Scotia: Applied Geomatics Research Group, Centre of Geographic Science .

Schmitt T.G., Schilling W., Sægrov S., Nieschulz K.-P. (2002). Flood risk management for urban drainage systems by simualtion and optimisation, In: 9th ICUD Conf., Portland.

Schmitt, T. G., Thomas, M., and Ettrich, N., 2004, Analysis and modelling of flooding in urban drainage systems, Journal of Hydrology, Vol. 299, pp 300-311.

Shan, J. and Shampath A., 2005. Urban DEM generation from raw LiDAR data: a labelling algorithm and its performance, Photogrammetric Eng. Remote sensing, 71(2), 217-226.

Shan J. and Sampath A., 2008. Building roof segmentation and reconstruction from LiDAR data point clouds using clustering techniques. International Archives of Photogrammetry, Remote Sensing and Spatial Information SciencesVol XXXVII. Part B3a, 279-284.

Sithole, G. and Vosselman, G. 2003: Report: ISPRS comparison of filters. Department of Geodesy, Faculty of Civil Engineering and Geosciences, Delft University of Technology, The Netherlands.

Stoker, J.M., Greenlee, S.K., Gesch, D.B. and Menig, J.C. 2006: CLICK: the new USGS center for LiDAR information coordination and knowledge. Photogrammetric Engineering and Remote Sensing 72, 613–16.

Tomičić B., Mark O. and Kronborg P. (1999). Urban flooding modelling study at Playa de Gandia. In: 3rd DHI Software Conf., HØrsholm.

Vosselmann, G., 2000. Slope-based filtering of laser altimetry data , Int. arch. Photogrammetry Remote Sensing, 33, Part B3/2, Amsterdam, the Netherlands, 935-942

Wack, R. and Wimmer, A. 2002: Digital terrain models from airborne laser scanner data – a grid based approach. International Archives of Photogrammetry, Remote Sensing and Spatial Information Sciences 34(3/B), 293–96.

Weidner, U. and Förstner W., 1995: Towards automatic building extraction from high resolution digital elevation models. ISPRS Journal of Photogrammetry and Remote Sensing, Vol. 4, pp 38-49.

Wu, C.S., and A.T. Murray, 2003. Estimating impervious surface distribution by spectral mixture analysis. Remote Sensing of Environment,84(4):493-505.

Zhang, K. and D. Whitmann, 2005. Comparison of three algorithms for filtering airborne LiDAR data, Photogrammetric Eng. Remote Sensing, 71(3), 313-324.